Localized Electronic States near Dislocations in Transition Metals

Hosson, J.Th.M. De

Published in:
International Journal of Quantum Chemistry

DOI:
10.1002/qua.560140841

Publication date:
1978

Localized Electronic States near Dislocations in Transition Metals

J. Th. M. DE HOSSON
Materials Science Centre, Rijksuniversiteit Groningen, Nijenborgh 18, Groningen, The Netherlands

Abstract

This article outlines a model for calculating the localized states of a ⟨100⟩ edge dislocation in Mo. The model used for the calculations is based on the multiple-scattering model (SCF-$X\alpha$-SW). The purpose of this investigation is (1) to determine changes in the electronic structure of the lattice near the core region of defects, where local changes in symmetry occur. How much does the electronic structure shift when one approaches a line defect from far away in the perfect region? (2) Several methods were developed to calculate the atomic configurations of defects by computer simulations. The influence of such procedures on the atomic positions was investigated. Several sets of positions were used to evaluate the sensitivity of electronic structure to interatomic distances. The highest occupied orbital energy level in the dislocated lattice is −0.441 Ry, while for the perfect lattice −0.531 Ry was found. This implies a small electronic field gradient around the dislocation line, and a corresponding redistribution of the electronic energies is obtained. The orbital energies show only a slight difference between the results obtained using atomic configurations determined by two computational procedures (0.002% of the total energy).

1. Introduction

The electronic states within condensed matter are of fundamental importance; in fact, no quantitative estimate of any property of a semiconductor, metal, or insulator on the basis of first principles can be done without information about these states.

In the past most of the investigations concerning the electronic states of dislocations were carried out for semiconductors [1–3]. The quantum mechanical consideration of such a complex system as a dislocation has been treated on the basis of more or less drastically simplified models. A theoretical study of the electrical effects of dislocations in the diamond-type lattice has been made by Read [4, 5]. The acceptor-type behavior is accounted for in terms of dangling bonds. The model identifies dislocation acceptors with the dangling unpaired electrons on the edge of the extra atomic plane of an edge dislocation. An electron paired with a dangling bond probably has less energy than a single free electron in the conduction band, but more than an electron in the valence band.

The presence of dislocations may notably increase the electrical resistivity of a metal. The change in electrical resistivity resulting from plastic deformation of metals has been measured by many workers [6–8], and several reviews on this subject have appeared. The most extended model known in the literature is the model of Huffman and Louat [9] for metals, which is based on the fact that dislocation motion in a metal induces an electric field which causes currents in

International Journal of Quantum Chemistry: Quantum Chemistry Symposium 12, 469–482 (1978)

0161-3642/78/0012-0469$01.00

the conduction electron gas. The concept of a large component of electronic drag which increases with decreasing temperature is used to give a qualitative explanation of the mechanical properties of bcc metals. Assuming, for measurements carried out at constant strain rate, that the dislocation velocity is, to a first approximation, independent of the temperature [10, 11], then the temperature dependence of the yield stress can possibly be ascribed to the electrical resistivity. According to Huffman and Louat, the temperature-dependent stress should be inversely proportional to the electrical resistivity. The fact that higher yield stresses occur in the lower-temperature range (especially in the case of bcc metals) can be explained by the influence of the temperature on the electronic drag component. Various attempts have been made to explain the discrepancy in metals between the theoretically predicted [12, 13] and the experimentally determined values [14, 15]; the latter appear to be 30 times greater than the former. The problem is caused by the fact that the localized electronic states within the core of the dislocation are not known. Harrison [16] assumed a hollow core consisting of a row of vacancies, which would seem to be physically implausible.

The present article will outline a model for calculations of these localized electronic states of an edge dislocation. The purpose of this investigation is twofold:

(1) It is to determine changes in the electronic structure of the lattice near the core region of defects, where local changes in symmetry occur. How much does the electronic structure shift when one approaches a line defect from far away in the perfect region?

(2) Several methods were developed to calculate the atomic configuration of the defects by computer simulations. The influence of such procedures on the atomic positions was calculated. Several sets of positions were used to evaluate the sensitivity of electronic structure to interatomic distances.

For the purpose of evaluating computer simulations for materials applications, the attempt is made in which the complex nature of the atomic configuration of extended defects often precludes calculation of the electronic properties of line defects in solids within the quantum mechanical frame.

A simple dislocation with ⟨100⟩ Burgers vector on a {100} slip plane in Mo is chosen because of the relatively high symmetry, necessary in connection with reduction of the eigenvalue problem yielding the electronic states. The model used for the calculations is based on the multiple-scattering model, originally used for polyatomic molecules, suggested by Slater [17] and further developed by Johnson [18]. This model has been extensively discussed in a recent review by Johnson [19]. The SCF–$X\alpha$–SW method has been thoroughly documented in other publications [20, 21], so that there is no need to describe the procedure here. In the present work the "muffin-tin" approximation was applied. The necessary input for the self-consistent-field scattered-wave model (SCF–$X\alpha$–SW) is the charge density at each point of a cluster of atoms. The charge density is the sum of the charge densities of individual atoms within the cluster. The calculations in the case of an individual molybdenum atom will be presented in Section 2 based on two methods: the Dirac–Slater formalism and the relativistic

Hartree–Fock–Slater formalism. In Section 3 the results for the electronic states of the perfect Mo lattice and the ⟨100⟩ edge dislocation are presented; they are followed by a discussion in Section 4.

2. Relativistic Dirac–Fock–Slater Calculations for Mo

As was mentioned in Section 1 the electronic density throughout the cluster of atoms is the starting point for the SCF-$X\alpha$-SW method. This electronic density is calculated from the initial set of spin orbitals within the $X\alpha$ exchange and is composed of relativistic wave functions. Two equations have been formulated for the total energy of a multielectronic problem: the Dirac–Slater (DS) equation and the Dirac–Hartree–Fock (DHF) equation [23].

A number of calculations with the DHF and the DS methods have appeared in recent years. The development of numerical computer programs to solve the DS [24] or DHF [25, 26] equations has led to a revival of interest in relativistic effects in atomic structure calculations.

For comparison the DS and DHF calculations in the case of molybdenum were carried out utilizing the program developed by Desclaux (in revised form) [25] for CYBER-74 equipment (DHF) and an analogous program which was given by Liberman et al. [24] (DS).

The statistical exchange parameter α in the case of molybdenum was chosen to be 0.7034. Although the value for α_{Mo} has not been given by Schwarz [27], the value for α_{Mo} has been extrapolated from the value of $\alpha_{Nb} = 0.7038$. The values of α within a given shell vary almost linearly with the atomic number Z, and always decrease.

The orbital energies calculated with DS and DHF are listed in Table I; for purposes of comparison, the Hartree–Fock (nonrelativistic) results, as computed with Froese-Fischer's program [28], are given too.

Although the differences between the orbital binding energies calculated by the DS and DHF methods are significant, the total energies (without the magnetic part in the case of DHF) are very close: −8095.278 and −8094.286 Ry, respectively.

The contribution of the magnetic part to the total energy is small: −0.067%. The total energy calculated by the HF method is −7950.694 Ry.

3. Self-Consistent-Field Scattered-Wave Calculations

A. Perfect Lattice of Mo

The space group symmetry O_h^9 is utilized for reduction of the eigenvalue problem. The cluster of one unit cell contains nine Mo atoms. A maximum L value of two was used for the decomposition of the wave function into spherical harmonics for all molybdenum spheres. Consequently, 90 functions have to be distributed over the irreducible representations in the O_h symmetry group (including the external sphere).

The muffin-tin radii were chosen in such a way that the interstitial region

TABLE I. Binding energies (negative) in rydberg units calculated by Dirac-Slater (DS), Dirac-Hartree-Fock (DHF), and nonrelativistic Hartree-Fock methods (HF) for molybdenum. (The asterisk means $j = 1 - 1/2$; if the asterisk is absent $j = 1 + 1/2$.)

SHELL	Dirac-Slater	Dirac-Hartree-Fock	Hartree-Fock
1 s	1455.645	1478.915	1442.746
2 s	205.8095	214.4052	206.0525
2 p	181.6984	188.6627	189.2361
2 p*	189.5353	196.5445	
3 s	35.03157	38.90492	37.51789
3 p	27.57801	30.65262	30.91952
3 p*	28.87119	31.99920	
3 d	16.30004	18.26604	18.91126
3 d*	16.54559	18.51812	
4 s	4.796017	5.859906	5.847546
4 p	2.833584	3.499782	3.738843
4 p*	3.020660	3.694136	
4 d	0.3278628	0.5881812	0.849683
4 d*	0.3426898	0.6031302	
5 s	0.3024247	0.4240948	0.454692

between the atomic spheres which touch each other is as small as possible. The corresponding atomic radius is 2.57 a.u. The Watson sphere radius was chosen to be 8.1 a.u. This value is slightly greater than the smallest value of the sphere enclosing the atoms, which is 7.8 a.u., but for comparing the orbital energies calculated for a perfect system with those of the dislocated system, equal values of the Watson radii were taken.

The charge density $\rho(\mathbf{r})$ within the cluster has been calculated using the Dirac–Slater formalism, where the Slater approximation for the exchange was utilized.

The first step in the self-consistent calculation is to determine the non-self-consistent option by computing the eigenvalues of the one-electron equations for a given potential, without performing the calculation of the charge density and the subsequent iteration to self-consistency. This non-self-consistent calculation solves the secular determinant for a preassigned range of energies and inverse interpolation for any zeros that may be found. The range of energies can be determined by the energies obtained from the atomic structure calculation. Because we are interested in the valence band only, this range determined lies between -0.1 and -1.1 Ry in the case of molybdenum.

The computational procedure iterates to self-consistency by calculating the

coefficients of the orbitals, "muffin-tin" averaging the total charge density, and generating a potential from it. In the calculations for molybdenum the charge densities of the atomic core electrons were kept fixed. The self-consistent iteration is continued to the point where the potential converges to the following value, which is dependent on the iteration:

$$\frac{V^B - V^E}{V^B} < 10^{-3}$$

V^B represents the potential at the beginning and V^E is the potential at the end.

In Table II the orbital energies (in rydbergs) are listed for the various irreducible representations in the O_h symmetry group. Figure 1 illustrates the sequence of the energy states which belong to the irreducible representations as listed in Table II.

In the case of a cluster of nine molybdenum atoms, 54 *d* electrons from the valence band have to be distributed over the irreducible representations. Indicating the highest occupied state as the Fermi state, the corresponding Fermi energy is, according to Table II, −0.513 Ry. The wave functions which correspond to the energy states as listed in Table II exhibit *d*-structure character and only a little admixture of the *s* character. The 5*s* orbital energies are lying too high for strong mixing, when using an integer number for occupation by electrons. Only the second state within the a_{1g} representation exhibits significant

TABLE II. Calculated orbital energies (in rydbergs). The occupation number is indicated in parentheses (all energies are negative).

Representation	Energy
a_{1g}	0.746 (2)
	0.573 (2)
	0.304 (0)
a_{2u}	0.441 (0)
	0.306 (0)
e_g	0.641 (4)
	0.585 (4)
	0.480 (0)
e_u	0.449 (0)
	0.429 (0)
t_{2u}	0.567 (6)
	0.526 (6)
t_{2g}	0.646 (6)
	0.526 (6)
	0.469 (0)
	0.404 (0)
	0.330 (0)
t_{1u}	0.581 (6)
	0.540 (6)
	0.513 (6)
	0.342 (0)
t_{1g}	0.491 (0)
	0.453 (0)

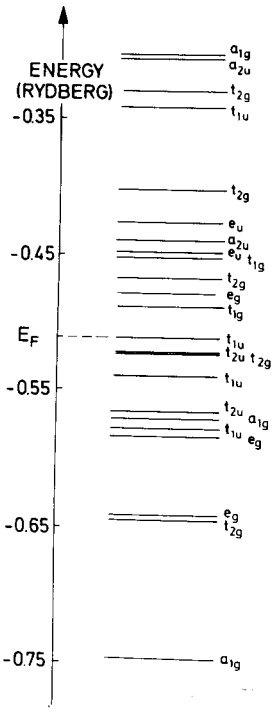

Figure 1. Energy levels of molybdenum.

mixing with s character. The nonoccupied orbital energy states in t_{1u} (−0.342 Ry), a_{1g} (−0.304 Ry), t_{2g} (−0.330 Ry), and a_{2u} (−0.306 Ry) also possess s character.

The total charge within the unit cell was determined by adding the charge on two molybdenum atoms and the interstitial charge. This charge was found to be 84.009 a.u., corresponding to a neutral charge on the unit cell.

B. ⟨100⟩ Edge Dislocation in Mo

The edge dislocation in Mo was introduced in the crystal by the method of Cotterill and Doyama [29]. Positions of the atoms are given by the displacements predicted by anisotropic elasticity theory [30]. Using the Johnson–Wilson interaction function for Mo [31] and the energy quench method of Bullough and Perrin [32], a relaxed atomic configuration was found as depicted in Figure 2.

The energy factor K [30] given by anisotropic elasticity theory was computed as 2.84 eV, which is close to the range of 2.86–2.90 eV found in the atomistic calculation. The corresponding core radius r_c, equivalent hole radius r_{eh}, and core energy E_{core} for this edge dislocation were r_c = 6.5–7.5 Å; r_{eh} = 3.0–3.4 Å; E_{core} = 1.8–2.1 eV. Several bond lengths and strains in the core are listed in Table III. The positions of the atoms A, B, . . . are indicated in Figure 2.

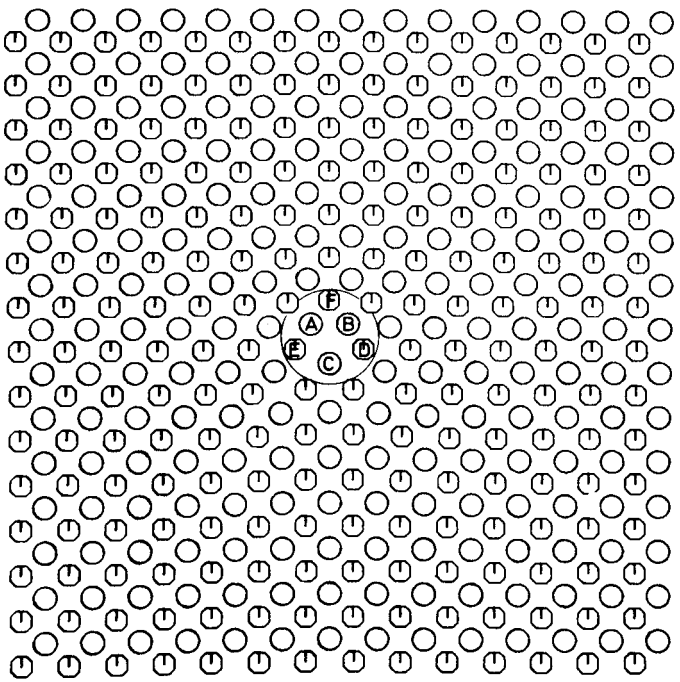

Figure 2. Two atomic layers projected on (001) plane of the atomic configuration of a [100] edge dislocation in molybdenum.

TABLE III. The bond lengths and strains (percents) within the core region of the [100] edge dislocation in Mo. For the numbering of sites, see Fig. 2.

	bond length (Å) (Bullough and Perrin method)	strains	variation (Sinclair's method)
A - B	2.587	-17.599	0.0062
A - F	2.661	- 2.149	0.0139
B - D	2.610	4.009	0.0028
D - E	4.733	50.729	0.0301
D - C	2.993	10.077	-0.0026

Sinclair [33] compared results of a calculation of bond length around a [100] edge dislocation with and without neglecting the higher-order terms in the displacement formulas. The variation in bond lengths obtained by the two methods is 1% for the *D–E*, 0.1% for *B–D*, and 0.4% for *A–B*. Assuming Sinclair's model for the higher terms, the variations in bond lengths calculated with this method are listed in Table III.

The two dislocation structures calculated using either the "energy quench" method or Sinclair's procedure will be distinguished in the following by DIS(I) and DIS(II), respectively.

The cluster containing nine molybdenum atoms involved in the electronic structure calculation is indicated in Figure 2. The symmetry properties of the dislocated system obey the C_{2v} symmetry group.

The muffin-tin radii in this structure were 2.46 a.u. Although other values for these radii might be chosen for reducing the interatomic space, these radii would be different among themselves; it is physically implausible to assume different radii for the same atom within a cluster. Therefore, this value was applied in both cases, DIS(I) and DIS(II).

For the two dislocation systems the charge density $\rho(\mathbf{r})$ as well as the orbital energies at the beginning of the self-consistent-field calculation obtained from a non-SCF run were calculated; the results showed that the difference between the two structures was of the order of magnitude of 0.01 Ry for various orbital energies. The same convergence criterion was operative as in the case of perfect Mo.

In Table IV calculated orbital energies are listed for both DIS(I) and DIS(II). Figure 3 illustrates the sequences of the orbital energies belonging to the various representations. The corresponding wave functions possess a pronounced d character. Three states with $5s$ character belong to the a_1 representation, two s states in b_1, two s orbitals in a_2, and two states possessing s character in b_2 representation. The energies were calculated in a_1 as -0.2338, -0.2337, and -0.2699 Ry. Only at the beginning of the SCF calculation were the $5s$ states involved, but no marked influence by them was observed.

Only the orbital energies indicated by DIS(I) are depicted in Figure 3 because of the slight differences between the states corresponding with DIS(I) and DIS(II).

In Table V the total energy E_T, the nucleus–nucleus interaction E_{NN}, the electron–nucleus energy E_{eN}, the electron–electron interaction E_{ee}, and the exchange energy E_{ex} are listed for both configurations.

4. Discussion

Only few investigations are reported in the literature concerning the electronic structure of molybdenum. Recently, Petroff and Viswanathan [34] calculated the density of states in W, Ta, and Mo from corresponding energy band structures obtained by a nonrelativistic APW calculation. This investigation was in good agreement with the calculation of the Fermi surfaces of Cr, Mo, and W by Loucks [35] and Mattheiss [36]. To find the Fermi energy level, the density-of-states curve is integrated. The Fermi level is that energy at which all the valence electrons are accounted for. The Fermi energies calculated by Petroff and Viswanathan and Loucks in the case of molybdenum are 0.498 and 0.542 Ry, respectively, as measured from the bottom of the lowest band.

Kress and Lapeyre [37, 38] investigated experimentally the electronic structure of the $4d$ metal molybdenum by photoemission and reflectance measurements. The data would indicate a filled d bandwidth of approximately 0.367 Ry and three peaks at $E - E_F = -0.037$, -0.118, and -0.287 Ry. A definite shoulder appears at $E - h\nu = -0.368$ Ry on the lower kinetic edge of the energy distribution curves for $h\nu > 0.735$ Ry. This shoulder persists within increasing photon energy and is taken to indicate the bottom of the $4d$ band in molybdenum.

TABLE IV. Calculated orbital energies (in rydbergs) (all energies are negative). The occupation number is indicated in parentheses.

Irreducible representation	DIS(I)	DIS(II)
a_1	0.597 (2)	0.597 (2)
	0.588 (2)	0.588 (2)
	0.581 (2)	0.583 (2)
	0.477 (2)	0.480 (2)
	0.467 (2)	0.460 (2)
	0.461 (2)	0.456 (2)
	0.457 (2)	0.452 (2)
	0.448 (2)	0.448 (2)
	0.445 (2)	0.445 (2)
	0.431 (0)	0.431 (0)
	0.377 (0)	0.377 (0)
	0.311 (0)	0.311 (0)
b_1	0.598 (2)	0.598 (2)
	0.475 (2)	0.478 (2)
	0.452 (2)	0.452 (2)
	0.444 (2)	0.445 (2)
	0.444 (2)	0.444 (2)
	0.429 (0)	0.431 (0)
	0.426 (0)	0.429 (0)
	0.425 (0)	0.426 (0)
	0.391 (0)	0.372 (0)
	0.365 (0)	0.351 (0)
	0.313 (0)	0.301 (0)
a_2	0.596 (2)	0.590 (2)
	0.487 (2)	0.458 (2)
	0.472 (2)	0.454 (2)
	0.459 (2)	0.445 (2)
	0.455 (2)	0.444 (2)
	0.444 (2)	0.443 (2)
	0.441 (2)	0.442 (2)
	0.429 (0)	0.430 (0)
	0.426 (0)	0.427 (0)
	0.321 (0)	0.317 (0)
	0.307 (0)	0.307 (0)
b_2	0.575 (2)	0.598 (2)
	0.491 (2)	0.478 (2)
	0.464 (2)	0.452 (2)
	0.459 (2)	0.445 (2)
	0.457 (2)	0.444 (2)
	0.449 (2)	0.432 (2)
	0.438 (0)	0.429 (0)
	0.435 (0)	0.426 (0)
	0.321 (0)	0.319 (0)
	0.317 (0)	0.309 (0)
	0.304 (0)	0.301 (0)

The three peaks found by photoemission study can be explained using Figure 1. A recorded energy of −0.037 Ry below the Fermi state corresponds to emission from the orbital energy lying around −0.55 Ry. The second band was predicted on the basis of photoemission measurements at −0.63 Ry, while the calculated orbitals lie at −0.64 Ry. The third emission should be from an energy state corresponding with −0.80 Ry. The lowest energy in our calculations is −0.751 Ry. In addition, Kress and Lapeyre gave a density of states above the Fermi energy based on optical reflectance studies and calculations. The strongest peak

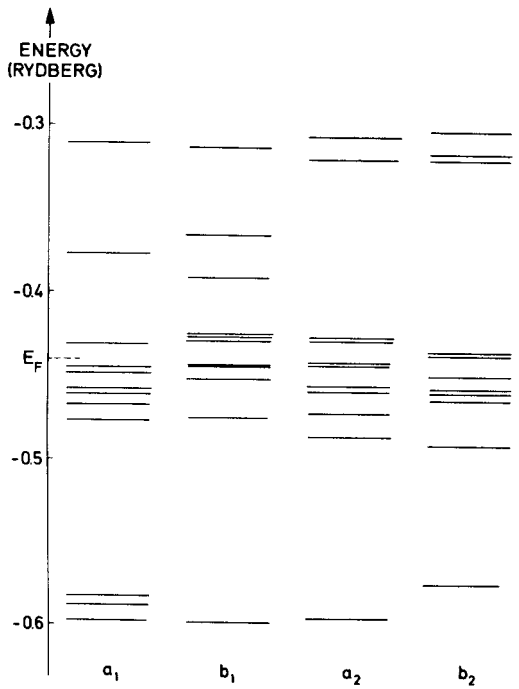

Figure 3. Orbital energies calculated for a ⟨100⟩ edge dislocation in molybdenum.

TABLE V. Calculated energies E_T, E_{NN}, E_{eN}, E_{ee}, and E_{ex} (in rydbergs).

	DIS(I)	DIS(II)
E_T	-73160.246	-73158.465
E_{NN}	18989.41	18994.91
E_{eN}	-214146.7	-214111.3
E_{ee}	51158.27	51119.73
E_{ex}	-2245.73	-2245.87

appeared 0.29 Ry above the Fermi level. This value agrees with the *s* states a_{1g}, lying 0.209 Ry above it.

In conclusion we can state that the results of the calculations agree with the experimental data given by Kress and Lapeyre regarding both the positions of the states below and above the Fermi level. Furthermore, the results from the calculations carried out with the SCF-$X\alpha$-SW method correspond well with those obtained by Petroff and Viswanathan, who also found three peaks for the density of states by the APW technique. The density of states calculated by Mattheiss [36] for W with APW functions again give three peaks. Since Mo and W have the same crystal structure and possess similar electronic configurations, the band structures are expected to be essentially the same (within an energy scale factor).

The orbital energies calculated for the ⟨100⟩ edge dislocation in molybdenum show only a slight difference between the results of the two methods of calculating the atomic configuration. The total energy E_T, the nucleus–nucleus interaction E_{NN}, and the electron–nucleus interaction E_{eN} are somewhat greater using Sinclair's method than the values obtained from the energy quench method of Bullough and Perrin (Table V). The differences can be expressed as percentages of E_T, E_{NN}, and E_{eN}: 0.002%, 0.029%, and 0.017%, respectively. From these values it can be concluded that the "improved" method as suggested by Sinclair for calculating the atomic configuration did not result in giving lower energy values in the electronic structure calculations. Furthermore, the longer computational time using Sinclair's method would seem to disqualify it from electronic structure investigations.

The highest occupied orbital in the case of DIS(I) is −0.441 Ry, while for the perfect lattice the value −0.513 Ry was found. However, the Fermi states E_F' [DIS(I)] and E_F have to be equal. The Fermi states E_F and E_F' can be equalized by either introducing a charge of $0.05e$ on the Watson sphere or by reducing the occupation number of the Fermi level from 2 to the fractional occupation number 1.98. The latter method implies a relative change which is less than in the former case because the relaxation of the "Slater transition state" formalism is taken into account, while the former actually implies only a shifting of the reference level. This small change in electronic occupation may be considered as a charge resulting from an electron density redistribution around the defect. In the case of the edge dislocation the electric neutrality cannot be determined in the same way as in the case of the perfect lattice by counting the charges on the atomic spheres and the interstitial spaces because of the lack of a unit cell. Of course, the dislocation configuration should be electrically neutral in metals. However, the supposition that neutral imperfections such as dislocations and point defects cannot produce electric field gradients due to a charge effect is in itself not valid. Roland [39] found that neutral impurities like silver in copper cause appreciable electric field gradients associated with a conduction electron charge density redistribution around the perfect centers. While in cubic metals the electric field gradients vanish at the lattice sites because of the cubic symmetry of those sites, imperfections such as dislocations may cause localized electric field gradients due to long-range strains, and spatially oscillating charge densities due to the conduction electron redistribution (charge effect). Close to the dislocation this redistribution will have the largest effect on the electric field gradients. Brown [8] has calculated the charge density associated with a dislocation in a free-electron metal to the first-order perturbation theory. He assumed that the isotropic elasticity theory described the atomic configuration of an edge dislocation, and Ogurtani and Huggins [40] did the same for a screw dislocation. It cannot be expected that the model correctly describes the situation within the core region. At large distances from the dislocation line the contribution to the charge shift from the electrons $\rho(\mathbf{r})$ had the view of $-0.025en_0$ (n_0 being the number of ions per unit volume) in Cu. Brown suggested that the average change in the magnitude of an electron wave function in the vicinity of the core is 0.05 and at large distances 0.01 of its unperturbed value. The total charge density varies

as $r^{-5/2}\sin(2k_F r + \pi/4)$ outside the core of the dislocation where k_F represents the wave factor at the free electron Fermi surface [k_F (molybdenum) = 2.2509 $\times 10^8$ cm^{-1}].

Although in our case the limited computed storage capacity compelled us to choose a cluster which is too small for considering the charge density behavior far from the dislocation (including the core), it may be concluded that the effect of the electron flow away from the dislocation is a minor one, which is in accordance with the suggestions given by Brown.

The redistribution of the electrons is evident from a comparison between Figures 1 and 3. In the perfect lattice 42 electrons are distributed over eight energy states within a range of 0.07 Ry, while the calculations for DIS(I) show that 42 electrons are distributed over 22 energy levels within a range of 0.05 Ry below the Fermi level.

The procedure outlined above supposes that the positions taken by the ions in the defect crystal are not influenced by the conduction electrons because the positions are calculated using an interatomic potential. However, any further relaxation of the atoms due to the conduction electron redistribution appears to be of secondary importance, as follows from the results of Brown.

The new model, used here to obtain the changes in orbital states for a dislocated lattice, can also be used to investigate the scattering of electrons by dislocation lines to formulate the expressions for the resistivity of dislocations. The wave function corresponding to a Hamiltonian of the imperfect lattice—which includes a perturbation potential—can be written for the region outside the core in terms of a disturbed Wannier function, while inside the core radius the solutions of the KKR method can be formulated. This has to be carried out carefully, in a manner analogous to the formulation given by Callaway [41] for the case of the scattering on point defects [42].

Another possible extension is to apply the SCF-$X\alpha$-SW method to determine the electronic states connected with dislocations in a semiconductor. Much more experimental data concerning the effect of plastic deformation on the electron mobility of dislocations in deformed germanium [43–47] are available than in metals [48, 49]. The advantage in calculating the electronic states connected with germanium using the SCF-$X\alpha$-SW method is the clear covalent bonding between the atoms in germanium in contrast to the metallic bonding in Mo. The problem in utilizing the SCF-$X\alpha$-SW procedure is the case of dislocations in diamond structures. Dislocations glide on (111) planes and have $[1\bar{1}0]$ as the Burgers vector. More atoms in nonequivalent positions have to be considered in the SCF-$X\alpha$-SW calculation to describe the dislocation than in metals. It would require a larger computer capacity and more computational time.

The quantum mechanical consideration of such a complex system as a dislocation should, of necessity, be based on more or less simplified models. The cluster method takes into account more correctly the atomic positions within the core region than other methods do and it furnishes more detailed information about the electronic states connected with a dislocation. In that way it provides a possible procedure to investigate the as yet unknown effects of electronic structure on phenomena such as Peierls barriers, stacking faults, and splitting

of dislocations, which all play an important role in physical problems derived from materials science.

Bibliography

[1] G. L. Pearson, W. T. Read, and F. J. Morin, Phys. Rev. **93,** 666 (1954).
[2] L. I. Kolesnik, Sov. Phys. Solid State **6,** 976 (1964).
[3] W. Bradley, *Progress in Semiconductors,* A. F. Gibson, Ed. (Heywood Comp. Ltd., London, 1960), p. 157.
[4] W. T. Read, Philos. Mag. **45,** 775 (1954).
[5] W. T. Read, Philos. Mag. **46,** 111 (1954).
[6] T. Holstein, Phys. Rev. **151,** 178 (1966).
[7] V. Ya. Kravchenko, Sov. Phys. Solid State **8,** 740 (1966).
[8] R, A. Brown, Phys. Rev. **141,** 568 (1966).
[9] G. P. Huffman and N. Louat, *Fundamental Aspects of Dislocation Theory,* J. A. Simmons, R. de Wit, and R. Bullough, Eds. (U.S. GPO, Washington, DC, 1970), NBS Spec. Publ. 317, vol. II, p. 1303.
[10] G. P. Huffman and N. Louat, Phys. Rev. Lett. **19,** 518 (1967).
[11] G. P. Huffman and N. Louat, Phys. Rev. Lett. **19,** 774 (1967).
[12] J. M. Ziman, *Electrons and Phonons* (Clarendon, Oxford, 1960), Sec. 6.5.
[13] S. C. Hunter and F. R. N. Nabarro, Proc. R. Soc. London Ser. A **220,** 542 (1953).
[14] L. M. Clareborough, M. F. Hargreaves, and M. H. Loretto, Philos. Mag. **7,** 115 (1962).
[15] J. G. Rider and C. T. B. Foxon, Philos. Mag. **13,** 289 (1966).
[16] W. A. Harrison, J. Phys. Chem. Solids **5,** 44 (1958).
[17] J. C. Slater, J. Chem. Phys. **43,** S228 (1965).
[18] K. H. Johnson, J. Chem. Phys. **45,** 3085 (1966).
[19] K. H. Johnson, Adv. Quantum Chem. **7,** 143 (1973).
[20] K. H. Johnson, J. G. Norman, and J. W. D. Connolly, *Computational Methods for Large Molecules and Localized States in Solids,* F. Herman, A. D. McLean, and R. K. Nesbet, Eds. (Plenum, New York, 1973), p. 161.
[21] K. H. Johnson, *Annual Review of Physical Chemistry,* H. Eyring, C. J. Christensen, and H. S. Johnston, Eds. (Annual Reviews, Palo Alto, CA, 1975), vol. 26, p. 39.
[22] J. C. Slater, Phys. Rev. **81,** 385 (1951).
[23] I. P. Grant, Adv. Phys. **80,** 747 (1970).
[24] D. A. Liberman, D. T. Cromer, and J. T. Waber, Comput. Phys. Commun. **2,** 107 (1971).
[25] J. P. Desclaux, Comp. Phys. Commun. **9,** 31 (1975).
[26] M. A. Coulthard, Proc. Phys. Soc. **91,** 44 (1967).
[27] K. Schwarz, Phys. Rev. **5,** 2466 (1972).
[28] C. Froese-Fischer, Comput. Phys. Commun. **1,** 151 (1969).
[29] R. M. J. Cotterill and M. Doyama, Phys. Rev. **145,** 465 (1966).
[30] J. P. Hirth and J. Lothe, *Theory of Dislocations* (McGraw-Hill, New York, 1964), p. 424.
[31] R. A. Johnson and W. D. Wilson, *Interatomic Potentials and Simulation of Lattice Defects,* P. C. Gehlen, J. R. Beeler, and R. I. Jaffee, Eds. (Plenum, New York, 1972), p. 301.
[32] R. Bullough and R. C. Perrin, Proc. R. Soc. London Ser. A **305,** 541 (1968).
[33] J. E. Sinclair, J. Appl. Phys. **42,** 5321 (1971).
[34] I. Petroff and C. R. Viswanathan, *Electronic Density of States,* L. M. Bennett, Ed. (U.S. GPO, Washington, DC, 1970), NBS Spec. Publ. 323, p. 53.
[35] T. L. Loucks, Phys. Rev. A **139,** 1181 (1965).
[36] L. F. Mattheiss, Phys. Rev. A **139,** 1893 (1965).
[37] K. A. Kress and C. J. Lapeyre, Rev. Sci. Instrum. **40,** 74 (1969).
[38] K. A. Kress and C. J. Lapeyre, *Electronic Density of States,* L. M. Bennett, Ed. (U.S. GPO, Washington, DC, 1971), NBS Spec. Publ. 323, p. 209.
[39] T. J. Roland, Phys. Rev. **119,** 900 (1960).
[40] T. O. Ogurtani and R. A. Huggins, Phys. Status Solidi **24,** 301 (1967).
[41] J. Callaway, *Quantum Theory of the Solid State* (Academic, New York, 1974), p. 371.

[42] J. Th. M. de Hosson, H. P. van de Braak, and W. J. Caspers, Phys. Lett. A **63,** 174 (1977).
[43] D. L. Dexter and F. Seitz, Phys. Rev. **86,** 964 (1952).
[44] R. A. Logan, G. L. Pearson, and D. A. Kleinman, J. Appl. Phys. **30,** 885 (1959).
[45] P. Haasen and W. Schröter, *Fundamental Aspects of Dislocation Theory,* J. A. Simmons, R. de Wit, and R. Bullough, Eds. (U.S. GPO, Washington, DC, 1970), NBS Spec. Publ. 317, p. 1231.
[46] B. Pödör, Phys. Status Solidi **16,** K167 (1966).
[47] E. Gerlach and M. Rautenberg, Phys. Status Solidi B **71,** K139 (1975).
[48] A. Hikata and C. Elbaum, Phys. Rev. Lett. **18,** 750 (1967).
[49] Z. S. Basinski and S. Saimoto, Can. J. Phys. **45,** 1161 (1967).

Received March 20, 1978